Anonymous Referee 1

We thank the reviewer for his detailed review and valuable comments. The manuscript has been modified according to the suggestions proposed by the reviewer. The remainder is devoted to the specific response item-by-item of the reviewer's comments

This paper describes a 3DCLOUD algorithm to generate stochastic 3D cloud fields to be used as a tool to understand cloud-radiation interactions. Overall, I found the paper to be a very good and thorough description of the 3DCLOUD algorithm and feel the paper is a nice fit for this journal. It is also wonderful that the authors provide a link to access the code described in this paper. My recommendation is to accept this paper after the minor points mentioned (below) are addressed.

Minor points:

1. **It would be helpful to reader to describe some fundamental differences between this 3DCLOUD generator and LES. While these may appear fairly obvious it would be nice to list them explicitly in the introduction and/or conclusions section for readers who are more familiar with LES and not so much stochastic cloud generators.**

In the introduction of the revised manuscript, we add before the sentence "Nevertheless, LES are very expensive to run in a 3D domain" this paragraph :

The goal of the LES approach is to simulate the three-dimensional atmospheric turbulent flows. There are different scales of turbulent eddies; large eddies (from 100 to 1000 m and more) that are produced directly by the instability of the mean flow and small eddies (from a few centimeters to 100 m) as well as by the energy-cascade process from the larger eddies (Moeng, 1984). LES seeks to capture accurately the larger eddies, while only modeling the smaller ones. Instead of reproducing all the scales of turbulence flow, they can integrate a flow in which small scale details are removed from the solution. The spatial filtered equations can, therefore, be integrated with available resources (Bryan et al., 2003). Nevertheless, they are still very expensive to run in a 3D domain.

Moreover, in section 2.1.1 (The simplification of basic atmospheric equation) we explain differences between LES equations and 3DCLOUD equations. After the presentation of the second law of newton, we add :

The continuity and momentum equations of the atmosphere under the anelastic and Boussinesq approximation, assuming shallow motion, neglecting Coriolis parameter, neglecting frictional forces, and neglecting the molecular viscosity can be written (Holton, 2004, p. 117 ; Houze, 1993, p. 35 ; Emanuel, 1994, p. 11)

$$\begin{cases} \nabla . \boldsymbol{u} = 0 \\ \dfrac{D\boldsymbol{u}}{Dt} = -\dfrac{1}{\rho_0}\nabla p^* + B\boldsymbol{k} \end{cases} \qquad (2)$$

where B is the buoyancy acceleration, ρ_0 is the constant mean value of air density and p^* is the pressure perturbations. The above differential operators are valid only in the limit when δt, δx, δy and δz approach 0 (Pielke, 2002, p. 41). Nevertheless, turbulent motions (shear induced eddies, convection eddies) have spatial and temporal variations at scales much smaller than those resolved by LES and 3DCLOUD. If we assume field variables can be separated in slowly varying mean field and rapidly varying turbulent component, and if we apply the Reynolds decomposition, we can rewrite the above equation set as:

$$\begin{cases} \nabla.\boldsymbol{u} = 0 \\ \dfrac{D\boldsymbol{u}}{Dt} = -\dfrac{1}{\rho_0}\nabla p^* + B\boldsymbol{k} + \boldsymbol{\Phi} \end{cases} \qquad (3)$$

where $\boldsymbol{\Phi}$ is the three dimensional convergence of the eddy flux of moment (Houze, 1993, p. 42), the turbulent flux (Holton, 2002, p 119) or the sub-grid correlation term (Pielke, 2002, p. 44). The Reynolds decomposition is not used in LES. The atmospheric equations are derived by spatial filtering, where a special function is applied. Thus, the filtering operation acts on atmospheric quantities and separates them in two categories: the resolved one (large eddy) and unresolved one (subgrid-scale). An unknown term remains in the filtered equations of LES, often called the subgrid-scale stress, which needs to be parameterized or estimated with the help of subgrid-scale modeling. This subgrid-scale stress for LES equations is analogous to the $\boldsymbol{\Phi}$ term for Reynolds decomposition. In 3DCLOUD, the $\boldsymbol{\Phi}$ term is voluntarily neglected. Indeed, the guiding idea of 3DCLOUD is to simulate, in the fastest way, 3D fluctuations of LWC/IWC of a cloud showing turbulent properties (or invariant scale properties).

For example, it would be nice if the authors would state how long it takes to run the matlab code for some of the cases at different spatial resolutions (perhaps in a table). Surely, it is much faster than LES.

This remark of referee 1 is analogous with one of the referee 2: “. What is the computational expense of 3DCloud as compared to LES?

In the revised manuscript, we add the Tab 1. We add this paragraph in section 4.1.1 (Effects of numerical spatial resolution):

Table 1 shows the time step, process time for one time step and process time for 2h-simulation with 3DCLOUD model, as a function of the numerical resolution. DYCOMS2-RF01 and BOMEX cases are presented. The process time for 2h-simulation is indicated because 3DCLOUD algorithm convergence is achieved after 2 h (or less) of simulation for stratocumulus, cumulus and cirrus regimes (see Fig. 10 for cumulus case). For both cases, the smaller the spatial resolution, the smaller the step time and the larger the process time. A comparison between 3DCLOUD and BRAMS LES computation time for a specific DYCOMS2-RF01 case is added (see Sect. 3.4). For this specific case, 3DCLOUD simulation is thirty times faster than BRAMS simulation. Note that 3DCLOUD (Matlab code) runs on a personal *computer with Intel Xeon E5520 (2.26 GHz) and BRAMS (Fortran code) runs on a PowerEdge R720 with Intel Xeon E5-2670 (2.60 GHz), both of them having a single-processor configuration.*

Table 1. Time step, process time for one time step and process time for 2h-simulation with 3DCLOUD model, as a function of the numerical resolution. DYCOMS2-RF01 and BOMEX cases are presented. A comparison between 3DCLOUD and BRAMS LES computation time for a specific DYCOMS2-RF01 case is added. 3DCLOUD (Matlab code) runs on a personal computer with Intel Xeon E5520 (2.26 Ghz) and BRAMS (Fortran code) runs on a PowerEdge R720 with Intel Xeon E5-2670 (2.60Ghz), both of them having a single-processor configuration.

Study case	Point mesh $N_x \times N_y \times N_z$	Horizontal numerical resolution Δx [m]	Time step [s]	Process time [s]	Process time for 2h-simulation [s]
DYCOMS2-RF01	$50 \times 50 \times 50$	200	10	0.4	290
	$100 \times 100 \times 50$	100	7	1.3	1340
	$200 \times 200 \times 50$	50	5	5	7200
	$400 \times 400 \times 50$	25	3	18	43200
BOMEX	$50 \times 50 \times 70$	200	30	0.7	170
	$100 \times 100 \times 70$	100	25	2.5	720
	$200 \times 200 \times 70$	50	20	10	3600
	$400 \times 400 \times 70$	25	14	40	20600
DYCOMS2-RF01					
3DCLOUD	$100 \times 100 \times 100$	40	13	2.7	1500
BRAMS	$100 \times 100 \times 100$	40	0.3	2	48600

2. **Figure 6, it is not clear to me which curve represents the 3DCLOUD generator. The figure caption states the bold curve but the color in the legend doesn't quite seem to correspond to the color of the bold curve.**

The legend of Figure 6 is modified in the revised manuscript in order to correspond to the color of the bold curve.

3. **3DCLOUD gen has been compared to time averaged LES profiles, which agree satisfactorily. Have the authors compared the simulated cloud fields (such as those shown in top row of fig. 7) to those produced by LES? If so do they also agree satisfactorily?**

This remark of referee 1 is analogous with one of the referee 2 : "How does the quality of results from 3DCloud compare to LES? Can the authors plot comparable scenes (planform snapshots of cloud or radiative fields) from LES in order to compare differences?".

In the revised manuscript, we add the following paragraph about the 3DCLOUD and LES cloud fields in the new section 3.4 entitled "Comparison between 3DCLOUD and BRAMS LES for DYCOM2-RF01 case":

In order to underscore differences between 3DCLOUD and LES for comparable scenes, we choose again the well documented DYCOMS2-RF01 case. Snapshots can be found, for example, in Stevens et al. (2005) and in Yamaguchi and Feingold (2012). We performed the 4h simulations of the DYCOMS2-RF01 case with 3DCLOUD and with the Brazilian Regional Atmospheric Modelling System (BRAMS v4) model (Pielke at al., 1992 ; Cotton et al., 2003). BRAMS simulations were provided by G. Penide (Penide et al., 2010). The BRAMS model is constructed around the full set of nonhydrostatic, compressible equations. The cloud microphysics parameterization is based on a two-moment scheme (Meyers et al., 1997). Subgrid scale fluxes are modeled following Deardroff (1980). The base calculations are performed on a $100 \times 100 \times 100$ *point mesh with a step time of 0.3 s.*

Figure 7 shows the instantaneous cloud-field snapshots of the pseudo albedo (see definition in Sect. 4) at four hours simulated by (a) the UCLA-0 model (picture taken from Stevens et al., 2005), (b) the BRAMS model, both configured following the DYCOMS2-RF01 case (Stevens et al., 2005) and (c) from 3DCLOUD with assimilation of meteorological profiles based on the DYCOMS-RF01 case. Both BRAMS and 3DCLOUD cases are drawn from simulations where $\Delta_x = \Delta_y = 40$ *m and* $\Delta_z = 12$ *m. These three snapshots of cloud fields are characterized by closed cellular convection with large cloud cover, as argued in Yamaguchi and Feingold (2012), who did simulation of DYCOMS-RF01 case with the LES mode of the Advanced Research WRF model. Figure 7 also shows the power spectra computed following the x and y directions and then averaged, for BRAMS and 3DCLOUD optical depth fields. The 3DCLOUD optical depth spectral slope is close to -5/3 in the* $[L_{out}: 1/(2\Delta x)]$ *m^{-1} wavenumber range, as expected, because of the statistical adjustment performed in the second step of the 3DCLOUD algorithm. By contrast, the BRAMS optical depth spectral slope is close to -5/3 only in the* $[2 \times 10^{-3}: 5 \times 10^{-3} \approx 1/(5\Delta x)]$ *m^{-1} wavenumber range. Depending on their degree of sophistication, LES do not always guarantee cloud invariant scale properties at the larger wavenumbers. Indeed, Bryan et al. (2003) have shown, that for the finite-difference model, the vertical wind velocity spectral slope is steeper than -5/3 for scales shorter than* $6\Delta x$. *Table 1 shows the computation performance of 3DCLOUD and BRAMS. For this specific case, 3DCLOUD simulation is thirty times faster than BRAMS simulation.*

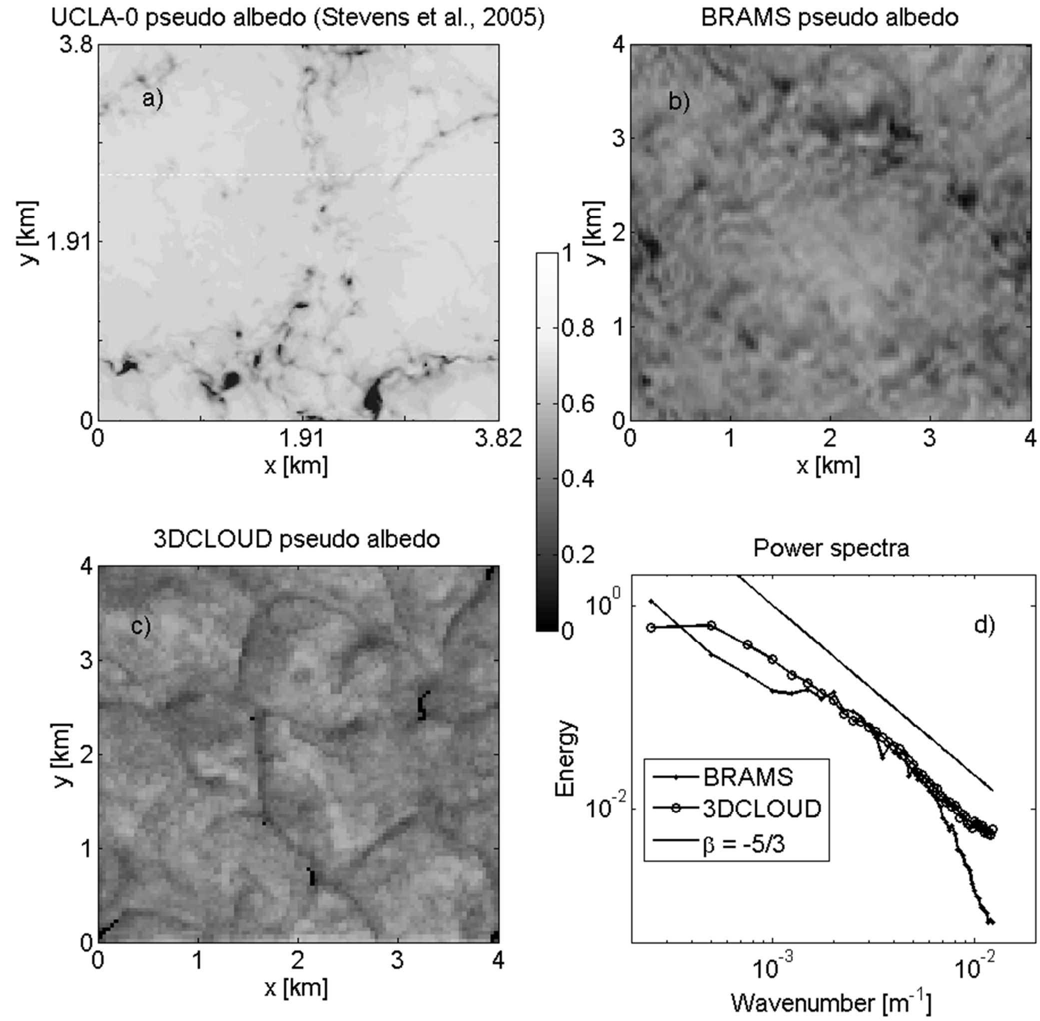

Figure 7. The instantaneous cloud-field snapshots of the pseudo albedo at four hours simulated by (a) the UCLA-0 model (picture taken from Stevens et al., 2005), (b) the BRAMS model, both configured following the DYCOMS2-RF01 case (Stevens et al., 2005) and (c) from 3DCLOUD with assimilation of meteorological profiles based on the DYCOMS-RF01 case. The UCLA-0 field is drawn from simulation where $N_x = N_y = 192$ *and* $\Delta_x = \Delta_y = 20$ *m. Both BRAMS and 3DCLOUD are drawn from simulations where* $N_x = N_y = N_z = 100$, $\Delta_x = \Delta_y = 40$ *m and* $\Delta_z = 12$ *m. Note that the 3DCLOUD field is obtained at the second step of the algorithm, with the inhomogeneity parameter* $\rho_\tau = 0.3$, *mean optical depth* $\bar{\tau} = 10$ *and* $L_{out} = 2$ *km. (d) is the optical depth power spectra computed following the x and the y directions and then averaged, for BRAMS (points) and 3DCLOUD (circles). A theoretical power spectrum with spectral slope* $\beta = -5/3$ *is added (black line).*

4. Figures 2 through 4, please state which cases are being examined in the figure captions.

In the revised manuscript, we add in the figure captions of figures 2 and figure 3 the sentence: *"Displayed is The DYCOM2-RF01 case is displayed*". We add in the figure captions of figure 4 and figure 5 the sentence: "*The BOMEX case is displayed*".

5. Throughout the paper there are frequent minor grammatical errors. In addition, some paragraph breaks (or lack of them) are awkwardly chosen.

The revised manuscript has been proofread by a native English speaker.

6. At the bottom of page 303 the authors state "This method gives satisfactory results for stratocumulus and cumulus clouds cloud fields but not for cirrus fields". A short explanation follow this statement of why it wouldn't work for cirrus fields would be helpful.

To control the cloud coverage C at the step 1 of 3DLOUD algorithm, we iteratively adjust the value of the vertical profile of vapor mixing ratio until C value reaches the required value within few percent. This method gives satisfactory results for stratocumulus and cumulus clouds fields but not for cirrus cloud fields.

To explain why it is difficult to control the cloud coverage in cirrus regime with the current version of 3DCLOUD, we add in the revised manuscript this paragraph, just after the sentence "This method gives satisfactory results for stratocumulus and cumulus clouds cloud fields but not for cirrus fields":

This is because condensation/evaporation and dynamic processes are different for stratocumulus/cumulus and cirrus regimes. Indeed, for liquid and warm stratocumulus/cumulus regime, liquid super or sub-saturation regions are not allowed in 3DCLOUD. Therefore, the distinction between cloudy and free cloud voxels is sharp. Moreover, as stratocumulus/cumulus fields are often driven by convection processes in a well-mixed planetary boundary layer, vertical correlation occurs between cloudy voxels (free cloud voxels) and updrafts (downdrafts). Thus, the fractional cloud coverage is easily controlled by adjusting the vertical profile of vapor mixing ratio during the simulation. By contrast, in ice cirrus regimes, (large) ice crystals can survive even if ice relative humidity is less than 100%. Ice super or sub-saturation regions are often observed in cirrus and are taken into account in the Starr and Cox parameterization used in 3DCLOUD. Therefore, many cloudy voxels still exist in our cirrus simulations, even if the ice water content is very small. The distinction between cloudy and free cloud voxels is, thus, very tenuous. Moreover, cirrus dynamics is often driven by wind shear: small fractional cloud coverage can exist at the top of the cirrus field due to convection or radiative cooling coexisting with large fractional cloud coverage and can also exist at the bottom of cirrus field due to wind shear. Finally, the total cloud coverage could be large. If we adjust the vertical profile of vapor mixing ratio during the simulation in the same way as for the stratocumulus/cumulus field, the total cloud *coverage will be difficult to control. Further investigations are thus needed to perfectly control the cloud coverage of cirrus simulated by 3DCLOUD.*

Anonymous Referee 2

We thank the reviewer for his detailed review and valuable comments. The manuscript has been modified according to the suggestions proposed by the reviewer. The remainder is devoted to the specific response item-by-item of the reviewer's comments.

General Comments:

Methods to compute three-dimensional effects of radiative transfer can be assessed if simulated test cloud fields (scenes) can be generated. This paper notes that there are two main methods to generate cloud fields: 1) large-eddy simulation (LES), and 2) stochastic models such as IAAFT (Venema et al. 2006) and Cloudgen (Hogan and Kew 2005). This paper proposes an intermediate two-step method, called 3DCloud, in which a cloud field is simulated by a simplified dynamical equation set, and then the cloud field is statistically adjusted in order to impose a prescribed standard deviation, power spectral slope, and other quantities. The manuscript displays examples of cumulus, stratocumulus and cirrus cloud fields generated by 3DCloud.
To my knowledge, 3DCloud is novel, and it produces plausible results in the examples, but it is unclear what are its advantages as compared to generating cloud fields using LES or existing stochastic models. In particular, it is not clear from the manuscript that 3DCloud is significantly less expensive than LES or significantly more accurate than existing stochastic models.

Specific Comments:

What are the advantages of the proposed method over IAAFT or Cloudgen? Is the main advantage accuracy of results?

3DCLOUD, like both IAFFT and Cloudgen models, is a stochastic cloud models and uses Fourier tools (manipulation of energy and phase in frequencies space) and amplitude adaptation (manipulation of distributions) in order to generate cloud fields. To answer to the general comments and to this question, we add a new section (2.3) entitled "Differences between 3DCLOUD, IAFFT and Cloudgen models":

Both IAAFT (Venema et al., 2006) and Cloudgen (Hogan and Kew, 2005) models are purely stochastic Fourier based approaches that are able to generate synthetic or surrogate cloud. On the contrary, 3DCLOUD solves, in a first step, basic atmospheric equations, in order to generate an intermediate cloud field. In its second step, as for both IAFFT and Cloudgen models, it uses Fourier tools (manipulation of energy and phase in frequency space) and amplitude adaptation (manipulation of distributions) in order to generate the final cloud field. IAAFT and Cloudgen are designed to simulate stratocumulus/cumulus fields for the first and cirrus fields for the second, when 3DCLOUD is able to simulate stratocumulus, cumulus and cirrus field within the same framework.

More specifically, the IAAFT method is designed to generate surrogate clouds having both the amplitude distribution and power of the original cloud (2D LWC from 1D LWP *measurement, 3D LWC from 2D LWC fields or 3D LWC from 3D fields generated by LES). It needs LES inputs or measurements. As explained in Venema et al. (2006), stratocumulus often display beautiful cell structures, similar to Bénard convection, and LES clouds show such features. But their 3D IAFFT surrogates show these much less and do not show fallstreak or a filamentous structure. Due to the specific manipulations of Fourier coefficients presented in the paper, we show that 3DCLOUD is able to simulate the cell structure of stratocumulus (see Fig. 7c and Fig. 8), the filamentous structure of cirrus (see Fig. 13) and the cirrus fallstreaks (see Fig. 14 and Fig. 15) relatively well. Moreover, the objective of 3DCLOUD is not to provide many surrogate clouds with the same amplitude distribution and power spectrum from an LES original cloud, but to provide 3D LWC (or optical depth) with the required cloud coverage, the -5/3 spectral slope (often observed in real clouds), the mean value of the gamma distribution of the optical depth and the inhomogeneity parameter, all these parameters being very pertinent for radiative transfer.*

Cloudgen is designed to simulate surrogate cirrus with the cirrus specific structural properties: fallstreak geometry and shear-induced mixing. It first generates a 3D fractal field by performing an inverse 3D Fourier transform on a matrix of simulated Fourier coefficients with amplitude consistent with observed 1D spectra. Then random phases are generated for the coefficient allowing multiple cloud realizations with the same statistical properties. Horizontal slices from the domain are manipulated in turn to simulate horizontal displacement and to change the spectra with height. The final field is scaled to produce the observed mean and fractional standard deviation of ice water content. 3DCLOUD does not use a 3D fractal field, but a 3D IWC field simulated by the simplified atmospheric equation set. Therefore, cloud structures due to wind shear are physically obtained by taking into account the advection (a nonlinear term in momentum equation) rather than by a linear horizontal displacement of phase. Afterwards, in the current version of 3DCLOUD, for each level, 2D horizontal slices of this 3D IWC are manipulated in 2D Fourier domain in such a way that the Fourier coefficient amplitude is consistent with the 2D spectra of the simulated IWC, with the constraint that the 1D spectral slope is equal to -5/3 (this value can be change easily in future version of 3DCLOUD). At each level, the 2D phase for the coefficient is kept unchanged. Finally, the mean value of the 3D IWC and the inhomogeneity parameter are adjusted. As explained by Hogan and Kew (2005), it is difficult with Cloudgen to generated anisotropic cirrus structure such as roll-like structure near cloud top. 3DCLOUD, using physically based equations, allows simulating such kinds of anisotropy, as for example, 3DCLOUD Kelvin-Helmholtz wave breaking (see Fig. 14).

On p. 298, lines 15–18, the manuscript states "The disadvantage of such model lies in that effects of meteorological processes are poorly considered and dominant scales of organization related to turbulent eddy due, for example, to wind shear, convection, entrainment are not considered." Although Cloudgen does consider the effect of wind shear on cirrus fall streaks, it is true that physical processes are not directly modeled by

the existing stochastic models. However, does 3DCloud produce more realistic cloud scenes?

We agree that the sentence “in stochastic model, wind shear, convection and entrainment are not considered” is too definitive. In the revised manuscript, we take account of the remark of the referee 2 and write:

The disadvantage of such models arises from the fact that effects of meteorological processes are not always considered and dominant scales of organization related to turbulent eddy due, for example, to wind shear, convection, and entrainment are not directly modeled. At the same time, it should be noted that Cloudgen does consider the effect of wind shear on cirrus cloud.

Looking empirically at the results, it is not clear to me that there is more realism, as compared to stochastic models, in 3DCloud’s stratocumulus (Sc) field depicted in Fig. 7 or the cumulus field depicted in Fig. 8. For instance, the Sc field appears to have smoother small scales than observed Sc clouds, …

3DCLOUD, as noted by the referee2 in his general comments, is an intermediate two-step method. Cloud fields are simulated by a simplified dynamical equation set and are then statistically adjusted. Cloud fields depicted in Fig. 7 and Fig. 8 (Fig. 8 and Fig. 9 in the revised manuscript) are obtained after the first step of 3DCLOUD. As explained further in our responses to referee 2, since dynamical equation set are very simplified, we do not expect that the 3D large spatial structures show the same turbulent properties as those observed in real cloud (especially the 1D spectral slope close to -5/3 of LWC/IWC). Therefore, cloud fields depicted in Fig. 7 and Fig. 8 (Fig. 8 and Fig. 9 in the revised manuscript) appears to have smoother small scales than the observed clouds which results in a 1D spectral slope often close to -2 or -3. Indeed, the 1D power spectrum of a stratocumulus cloud after the first step plotted in Fig 10e (Fig. 12e in the revised manuscript) has a spectral slope larger (absolute value) than the desired 1D spectral slope of -5/3. The statistical adjustment of the 1D spectral slope close to -5/3 is done in the second step.

… and the simulation doesn’t have a large enough domain to contain power in the mesoscale.

The referee 2 is right. In the revised manuscript, in section 2.1.1 (The simplification of basic atmospheric equations), we add :

As the horizontal extension of the simulated cloud fields is around a few km, horizontal pressure is assumed to be constant. Therefore, the current version of 3DCLOUD does not have a large enough domain to contain power in the mesoscale.

Also, the spacing between Cu clouds seems to grow closer as the resolution is refined, and it is unclear whether the cloud spacing converges at high resolution.

In the revised manuscript, we add the following figure and text in section 4.1.1 (Effects of numerical spatial resolution):

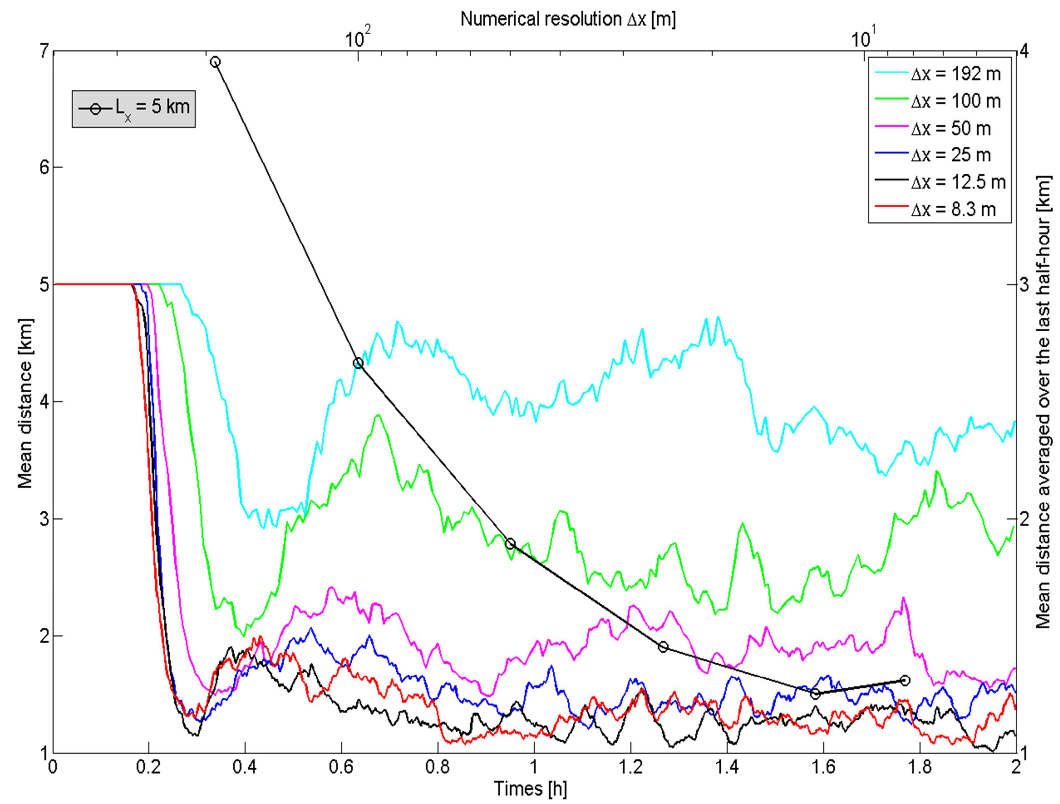

Figure 10. Time series of the mean distance between cloud areas for different horizontal numerical spatial resolutions (colored lines) with a constant vertical numerical spatial resolution ($\Delta z = 38.5$ m) and mean distance averaged over the last-half hour of a 2h simulation as a function of numerical spatial resolution (black line with circles). The cumulus cloud is simulated by 3DCLOUD with assimilation of meteorological profiles based on the BOMEX case. Horizontal extensions are $L_x = L_y = 5$ km and vertical extension is $L_z = 2700$ m.

In addition, it is expected for the BOMEX case, that cloud spacing converges at high spatial resolution. In order to investigate it, we defined an estimator of the cloud spacing called the mean distance D_{mean}. To compute D_{mean} , the 3D LWC is vertically projected on the 2D x-y plan in order to obtain the 2D binary image of the cloud coverage with free cloud areas set to 0 and cloudy areas set to 1. Then we compute the mean distance between the cloud cell for the x and y directions to obtain D_{mean}. Figure 10 shows time series of D_{mean} for different horizontal spatial resolution ($\Delta x = \Delta y =$ 192, 100, 50, 25, 12.5 and 8.3 m) with a constant vertical resolution ($\Delta z = 38.5$ m), for cumulus cloud fields simulated by 3DCLOUD after assimilation of the BOMEX case meteorological profiles. The main difference between these simulations and the BOMEX case simulation is the smaller horizontal extension $L_x = L_y = 5$

km instead of 10 km in order to access high numerical spatial resolution $\Delta x = 8.3$ m ($N_x = N_y = 600$, $N_Z = 70$). Cumulus clouds appear 10 to 20 min after the beginning of the simulation. After 1 h of simulation, D_{mean} is relatively constant with time, meaning that 3DCLOUD has converged. The mean distance averaged over the last half-hour of the 2h simulation $\overline{D_{mean}}$, is also presented in Fig. 10 as a function of the numerical spatial resolution Δx. $\overline{D_{mean}}$ is relatively constant for a spatial resolution Δx smaller than 20 m, showing that BOMEX cloud spacing converges for spatial resolution close to $\Delta x = 10$ m, a value smaller than $\Delta x = 25$ m used in Fig. 9d.

Furthermore, Cu in the BOMEX case are not organized by shear, and hence this aspect of organization cannot be tested. Can the authors compare with stochastic models or at least point to comparable plots by stochastic models in the literature? (Also, it would be nice to have metrics by which to compare the model results, but perhaps that is beyond the scope of this manuscript.)

We fully agree with this comment: "Cumulus in the BOMEX case are not organized by shear, and hence this aspect of organization cannot be tested". Even through it was not the main objective of the paper, we investigate briefly in the revised paper the aspect of cloud organization due to wind shear with 3DCLOUD model and with other stochastic models in the literature.

We add in the revised manuscript, in the new section 4.2.2 (Cirrus field and wind shear) the following paragraph:

We investigate briefly the aspect of cloud organization due to wind shear with 3DCLOUD model and with other stochastic models. We focus on the work of Marsham and Dobbie (2005) and of Hogan and Kew (2005). These two studies are very pertinent together. Indeed, based on RADAR retrievals of IWC from the Chilbolton 94 GHz RADAR on 27 December 1999, which shows a strongly sheared ice cloud (named hereafter RC99 case), Marsham and Dobbie (2005) investigated shear effects by simulating the RC99 case with the UK Met office LES. In contrast, Hogan and Kew (2005) used their Cloudgen model, a 3D stochastic cloud model being able to simulate the structural properties of ice clouds. To configure 3DCLOUD in order to simulate the RC99 case, we assimilate meteorological profiles (potential temperature, horizontal wind velocity) based on those drawn in Fig 2 in Marsham and Dobbie (2005). We run also the RC99a case with no wind (and therefore no wind shear), and the RC99b case where the potential temperature profile (drawn in Fig 15 in Marsham and Dobbie, 2005) reduces atmospheric stability in order to give more extensive Kelvin-Helmholtz wave braking. All our simulations are done with $N_x = N_y = 200$ and $N_z = 66$ and $\Delta_x = \Delta_y = 250$ m and $\Delta_z = 120$ m. Horizontal extensions are $L_x = L_y = 50$ km and vertical extension is $L_z = 8$ km between 4 km and 12 km. Note that 3DCLOUD, Marsham and Dobbie (2005) and Hogan and Kew (2005) numerical resolution are $\Delta_x = \Delta_y = 250$ m, $\Delta_x = 100$m and $\Delta_x \approx 780$ m, respectively. Note also that 3DCLOUD, Marsham and Dobbie (2005) and

Hogan and Kew (2005) horizontal extensions are $L_x = L_y = 50\,km$, $L_x = 50\ \ km$ and $L_x = L_y = 200\,km$.

Figure 14 shows a 2D vertical slice of 3DCLOUD IWC at an angle parallel to the wind of the RC99a case, the RC99 case and the RC99b case. Note that the 3DCLOUD fields are smooth because they are obtained at the first step of the algorithm. These three snapshots are very similar to those presented in Marsham and Dobbie (2005), allowing us to confirm that our basic atmospheric equations are correctly solved. In Fig. 14a, we can see small structures (few km) at above 7 km, due to radiative cooling at the cloud top and latent heat release in the updraughts. Below, we can observe fallstreaks advected (or not if there is no wind) relative to their source in the convective layer by the shear. The shear homogenizes the fallstreaks. Figure 14b clearly shows that 3DCLOUD simulations at the first step of the algorithm homogenize the fallstreaks a lot, certainly too much compared to the RADAR retrievals of IWC from the Chilbolton 94 GHz RADAR on 27 December 1999 (see Fig. 1 in Hogan and Kew, 2005). Figure 14c shows the RC99b case where 3DCLOUD model is able to simulate Kelvin-Helmholtz wave breaking, a dynamic aspect difficult to simulate with purely stochastic models.

Figures 15a and 15b are the same as Fig. 14b but 3DCLOUD fields are obtained at the second step of the algorithm, with 1D spectral slope close to -5/3 from the outer scale $L_{out} = 15$ km to the numerical scale $\Delta x = 250$ m. In Fig. 15a, the mean value of 3D IWC $\overline{IWC} = 0.07$ gm^{-3} and inhomogeneity parameter $\rho_{IWC} = 0.4$ for cloudy voxels are those computed from the 3D IWC field obtained at step one of the 3DCLOUD algorithm. In Fig. 15b, inhomogeneity parameter ρ_{IWC} is a function of height. Its values are roughly estimated from the Fig. 2c in Hogan and Kew (2005). Compared to Hogan and Kew (2005) simulations, 3DCLOUD snapshots show more details in the convective layer above 7 km as it simulates relatively well the convective cloud structures thanks to imposed numerical spatial resolution. By contrast to Fig. 15a, Hogan and Kew (2005) simulations show more details in the layer under 7 km, where the shear-induce mixing is important. In order to obtain such details in the layer under 7 km with 3DCLOUD, we have to constrain it with ancillary data: those provided by the RADAR retrievals of IWC and shown on Fig. 2c in Hogan and Kew (2005). Indeed, if we force, in the second step of 3DCLOUD algorithm, the vertical inhomogeneity parameter to match the one estimated crudely from the RADAR retrievals, we obtain Fig. 15b. Details in the layer under 7 km of this snapshot are quite similar to those obtained by Hogan and Kew (2005).

Finally, Fig. 16, which is similar to Fig. 2 in Hogan and Kew (2005), shows vertical profiles of the cloud fraction, the mean of logarithm of IWC for the cloudy voxels and the standard deviation of logarithm of IWC for cloudy voxels computed from two 3DCLOUD fields obtained at the second step of the algorithm for RC99 case. As for Fig. 15, inhomogeneity parameter is $\rho_{IWC} = 0.4$ for the first cloud field and depends on height and it is derived from RADAR retrievals for the second case. For both cloud fields, the cloud coverage is equal to 1 between 5 km and 10 km. RADAR retrievals of IWC shows that the cloud coverage is equal to 1 only *between 5.5 km and 7 km, and decreases to 0 at 10 km. However, as discussed in Sect. 2.1.2, the current version of 3DCLOUD is not able to readily simulate fractional cloud coverage in the cirrus regime. For both cloud fields, vertical profiles of the mean IWC are quite similar and consistent with those retrieved from RADAR. The inhomogeneity parameter vertical profile simulated by the current version of 3DCLOUD is too small, leading to a smoothing of the layer under 7 km that can be improved if the vertical profile of the inhomogeneity parameter is known.*

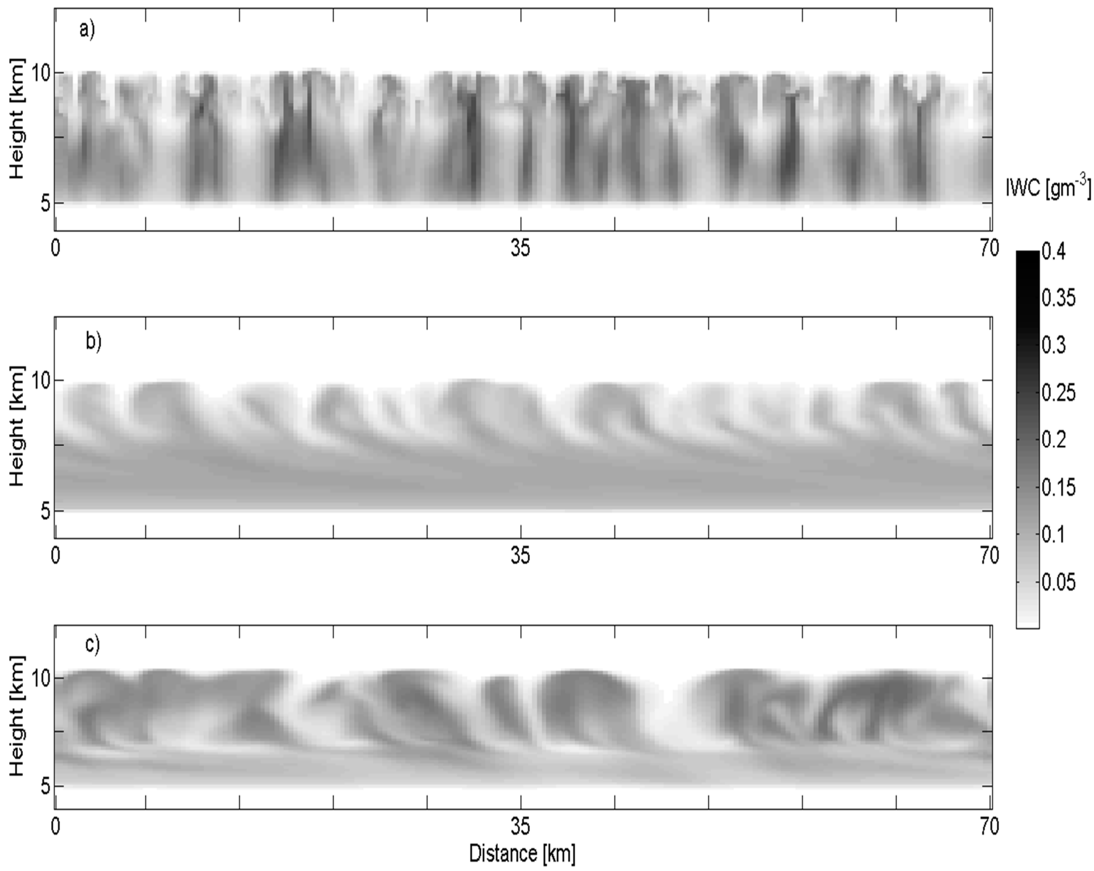

Figure 14. 2D vertical slice of 3DCLOUD ice water content (IWC gm^3) through a 3D simulation at an angle parallel to the wind (a) RC99a case, (b) RC99 case and (c) RC99b case. Fields are obtained from simulations where $N_x = N_y = 200$ and $N_z = 66$ and $\Delta_x = \Delta_y = 250$ m and $\Delta_z = 120$ m. Horizontal extensions are $L_x = L_y = 50$ km and vertical extension is $L_z = 8$ km between 4 km and 12 km. Note that the 3DCLOUD fields are smooth because obtained at the first step of the algorithm.

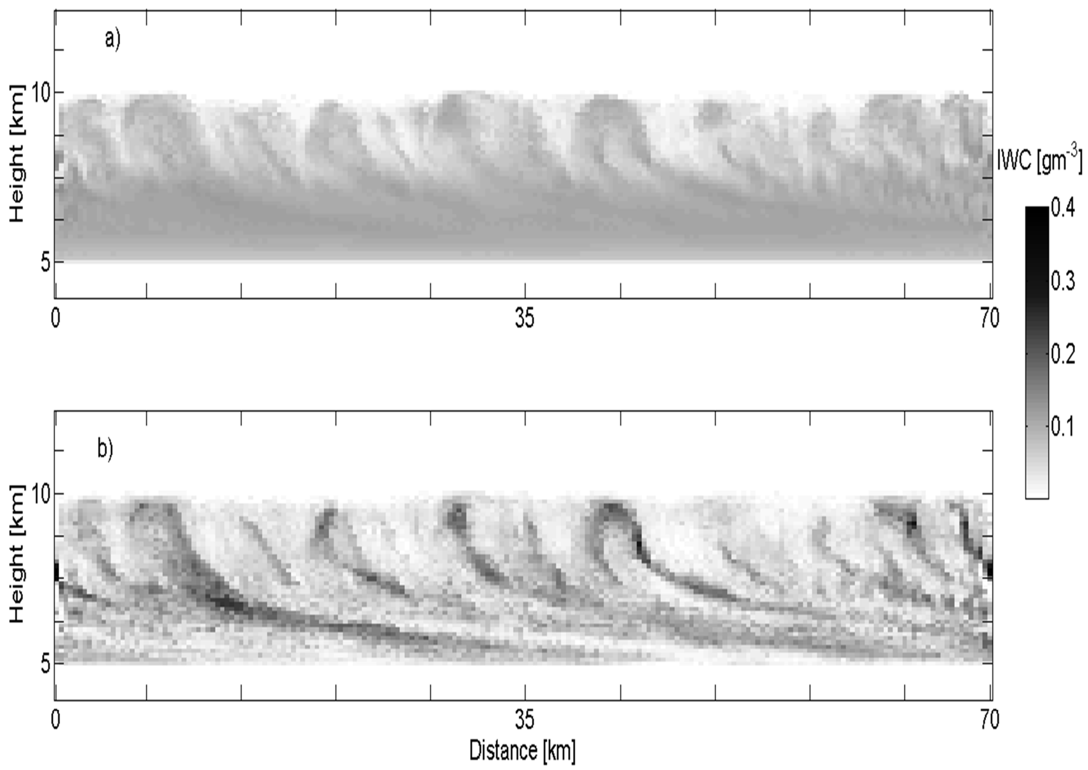

Figure 15. Same as Fig. 14b but after the second step of the algorithm, where 1D spectral slope is close to -5/3 from outer scale $L_{out} = 15$ km to the numerical scale $\Delta x = 250$ m.(a) mean of 3D IWC is $\overline{IWC} = 0.07$ gm^{-3} and inhomogeneity parameter $\rho_{IWC} = 0.4$ for cloudy voxels. (b) same as (a) but with inhomogeneity parameter ρ_{IWC}, function of height and derived from the 27 December 1999 RADAR measurements between 10 and 12 UTC crudely estimated from the Fig. 2c in Hogan and Kew (2005).

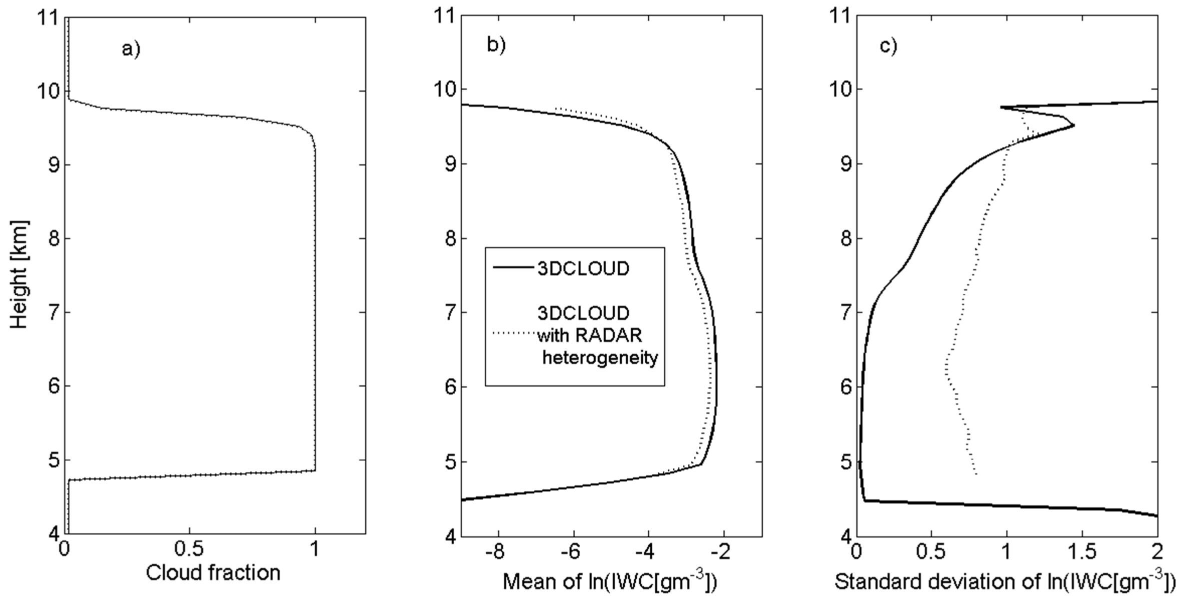

Figure 16. Vertical profiles for the RC99 case of (a) cloud fraction, (b) mean of ln(IWC) for the cloudy voxels and (c) standard deviation of ln(IWC) for cloudy voxels computed from two 3DCLOUD fields obtained at the second step of the algorithm. The solid lines indicate simulation where inhomogeneity parameter is $\rho_{IWC} = 0.4$ and the dotted lines indicate simulation where the parameter ρ_{IWC}, function of height, is derived from the 27 December 1999 RADAR measurements between 10 and 12 UTC and crudely estimated from the Fig 2c in Hogan and Kew (2005).

Thinking more about the theory, we see that in the equation set (5), the momentum equation is missing a pressure term and a turbulent diffusion term. It is not clear to me that, without these terms, wind shear, convection, and entrainment can be accurately modeled. Can the authors give some justification?

The continuity and momentum equations of the atmosphere under the anelastic and Boussinesq approximation, assuming shallow motion, neglecting Coriolis parameter, neglecting frictional forces, and neglecting the molecular viscosity can be written (Holton, 2004, p. 117 ; Houze, 1993, p. 35 ; Emanuel, 1994, p. 11)

$$\begin{cases} \nabla.\mathbf{u} = 0 \\ \dfrac{D\mathbf{u}}{Dt} = -\dfrac{1}{\rho_0}\nabla p^* + B\mathbf{k} \end{cases}$$

where $\mathbf{u}$ is the wind velocity vector, B is the buoyancy acceleration, ρ_0 is the air density and p^* is the pressure perturbations. We agree with referee 2 that a pressure term in equation set (5) (6 in the revised manuscript) is missing. We added it in the equation sets in the revised manuscript.

The above differential operators are valid only in the limit when δt, δx, δy and δz approach 0 (Pielke, 2002, p. 41). Nevertheless, turbulent motions (shear induced eddies, convection eddies) have spatial and temporal variations at scales much smaller than those resolved by LES (Holton, 2002, p. 115) and 3DCLOUD. If we assume field variables can be separated into slowly varying mean field and rapidly varying turbulent component, and if we apply the Reynolds decomposition, we can rewrite the above equation set as :

$$\begin{cases} \nabla.\mathbf{u} = 0 \\ \dfrac{D\mathbf{u}}{Dt} = -\dfrac{1}{\rho_0}\nabla p^* + B\mathbf{k} + \boldsymbol{\mathcal{F}} \end{cases}$$

where $\boldsymbol{\mathcal{F}}$ is the tree dimensional convergence of the eddy flux of moment (Houze, 1993, p. 42) or the turbulent flux (Holton, 2002, p 119) or the sub-grid correlation term (Pielke, 2002, p. 44). Reynolds decomposition is not used in LES. The atmospheric equations are derived by spatial filtering, where a special function is applied. In doing thus, the filtering operation acts on atmospheric quantities and separates them to the resolved one (large eddy) and unresolved one (subgrid-scale). It remains into the filtered equations of LES an unknown term, often called the subgrid-scale stress, needed to be parameterized or estimated with the help of subgrid-scale modeling. This subgrid-scale stress for LES equations is analogous to the $\boldsymbol{\mathcal{F}}$ term for Reynolds decomposition.

It is not clear for us, but we assume that the referee 2 call $\boldsymbol{\mathcal{F}}$ the “turbulent diffusion term”.

In 3DCLOUD, the $\boldsymbol{\mathcal{F}}$ term is voluntary neglected. Indeed, the guiding idea of 3DCLOUD is to simulate, in the fastest way on personal computer, 3D fluctuations of liquid/solid water content (3D LWC/IWC) of a cloud that shows turbulent properties (or invariant scale properties). To do this, in the first step of 3DCLOUD algorithm, 3D large spatial structures of cloud are simulated with the help of the very simplified Navier-Stokes and thermodynamical equations. Because these equations are very simplified (in order to make fast 3DCLOUD algorithm), we do expect that the 3D large spatial structures simulated at first step not show the turbulent properties as those observed in real cloud (especially the 1D spectral slope close to -5/3 of LWC/IWC), as pointed out by referee 2 in his above remark: “the field appears to have smoother small scales than observed clouds”. However, 3D relatively complex spatial shapes due to convection motions, to wind shear (Kelvin-Helmholtz wave, an example added in the revised manuscript) are relatively well simulated at the first step of the 3DCLOUD algorithm. Moreover, because Navier-Stokes and thermodynamical equations are very simplified, because algorithm used a Fourier projection method to force free wind divergence and do not compute explicitly the pressure perturbation with the help of Poisson equation, 3DCLOUD is, of course, faster than LES (we give in the revised manuscript an example where 3DCLOUD is thirty times faster than the BRAMS LES). In the second step of 3DCLOUD, stochastic methods based on Fourier tools are used to correct the smoother small scales of cloud. Especially, the 1D spectral slope of LWC/IWC is forced to be close to -5/3 by keeping unchanged the 3D large spatial structures simulated at first step. By the way, statistical parameter pertinent to radiative transfer (mean, inhomogeneity parameter) can be adjusted by the user.

In doing so, 3DCLOUD will never models **very** **accurately** entrainment, which is a difficult task, even if LES is used (spatial numerical resolution must be small (Stevens et al., 2002 ; Bryan et al., 2003) and therefore simulations are computational time expensive). However, 3DCLOUD gives the opportunity to a user who is not a specialist of LES, under Matlab environment with a personal computer, to simulate, quite rapidly, 3D larges structures of clouds (stratocumulus, fairly weather cumulus and cirrus) showing invariant scale properties as observed in real clouds.

We did modifications though the revised manuscript in order to clarify the "philosophy" of 3DCLOUD, its position compared to LES and stochastic models, and the simplification of equations of basic atmospheric equations used in 3DCLOUD algorithm.

2. How does the quality of results from 3DCloud compare to LES? Can the authors plot comparable scenes (planform snapshots of cloud or radiative fields) from LES in order to compare differences?

This remark of referee 2 is analogous with one of the referee 1 : "3DCLOUD gen has been compared to time averaged LES profiles, which agree satisfactorily. Have the authors compared the simulated cloud fields (such as those shown in top row of fig. 7) to those produced by LES? If so do they also agree satisfactorily?"

In the revised manuscript, we add the following paragraph about the 3DCLOUD and LES cloud fields in the new section 3.4 entitled "Comparison between 3DCLOUD and BRAMS LES for DYCOM2-RF01 case":

In order to underscore differences between 3DCLOUD and LES for comparable scenes, we choose again the well documented DYCOMS2-RF01 case. Snapshots can be found, for example, in Stevens et al. (2005) and in Yamaguchi and Feingold (2012). We performed the 4h simulations of the DYCOMS2-RF01 case with 3DCLOUD and with the Brazilian Regional Atmospheric Modelling System (BRAMS v4) model (Pielke at al., 1992 ; Cotton et al., 2003). BRAMS simulations were provided by G. Penide (Penide et al., 2010). The BRAMS model is constructed around the full set of nonhydrostatic, compressible equations. The cloud microphysics parameterization is based on a two-moment scheme (Meyers et al., 1997). Subgrid scale fluxes are modeled following Deardroff (1980). The base calculations are performed on a $100 \times 100 \times 100$ *point mesh with a step time of 0.3 s.*

Figure 7 shows the instantaneous cloud-field snapshots of the pseudo albedo (see definition in Sect. 4) at four hours simulated by (a) the UCLA-0 model (picture taken from Stevens et al., 2005), (b) the BRAMS model, both configured following the DYCOMS2-RF01 case (Stevens et al., 2005) and (c) from 3DCLOUD with assimilation of meteorological profiles based on the DYCOMS-RF01 case. Both BRAMS and 3DCLOUD cases are drawn from simulations where $\Delta_x = \Delta_y = 40$ *m and* $\Delta_z = 12$ *m. These three snapshots of cloud fields are characterized by closed cellular convection with large cloud cover, as argued in Yamaguchi and Feingold (2012), who did simulation of DYCOMS-RF01 case with the LES mode of the Advanced Research WRF model. Figure 7 also shows the power spectra computed following the x and y directions and then averaged, for BRAMS and 3DCLOUD optical depth fields. The 3DCLOUD optical depth spectral slope is close to -5/3 in the* $[L_{out}: 1/(2\Delta x)]$ *m^{-1} wavenumber range, as* *expected, because of the statistical adjustment performed in the second step of the 3DCLOUD algorithm. By contrast, the BRAMS optical depth spectral slope is close to -5/3 only in the* $[2 \times 10^{-3} : 5 \times 10^{-3} \approx 1/(5\Delta x)]$ *m^{-1} wavenumber range. Depending on their degree of sophistication, LES do not always guarantee cloud invariant scale properties at the larger wavenumbers. Indeed, Bryan et al. (2003) have shown, that for the finite-difference model, the vertical wind velocity spectral slope is steeper than -5/3 for scales shorter than* $6\Delta x$. *Table 1 shows the computation performance of 3DCLOUD and BRAMS. For this specific case, 3DCLOUD simulation is thirty times faster than BRAMS simulation.*

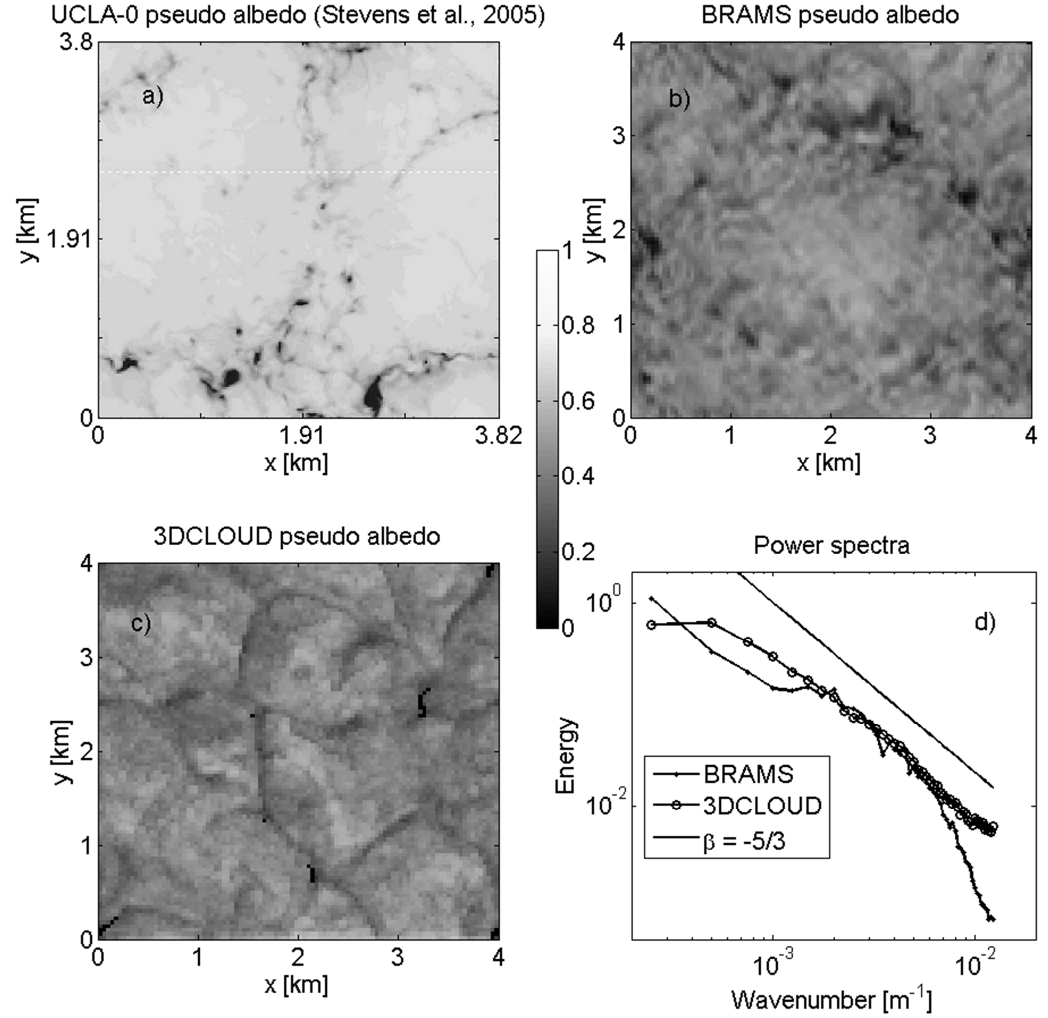

Figure 7. The instantaneous cloud-field snapshots of the pseudo albedo at four hours simulated by (a) the UCLA-0 model (picture taken from Stevens et al., 2005), (b) the BRAMS model, both configured following the DYCOMS2-RF01 case (Stevens et al., 2005) and (c) from 3DCLOUD with assimilation of meteorological profiles based on the DYCOMS-RF01 case. The UCLA-0 field is drawn from simulation where $N_x = N_y = 192$ *and* $\Delta_x = \Delta_y = 20$ *m. Both BRAMS and 3DCLOUD are drawn from simulations where* $N_x = N_y = N_z = 100$*,* $\Delta_x = \Delta_y = 40$ *m and* $\Delta_z = 12$ *m. Note that the 3DCLOUD field is obtained at the second step of the algorithm, with the inhomogeneity parameter* $\rho_\tau = 0.3$*, mean optical depth* $\bar{\tau} = 10$ *and* $L_{out} = 2$ *km. (d) is the optical depth power spectra computed following the x and the y directions and then averaged, for BRAMS (points) and 3DCLOUD (circles). A theoretical power spectrum with spectral slope* $\beta = -5/3$ *is added (black line).*

3. What is the computational expense of 3DCloud as compared to LES?

This remark of referee 2 is analogous with one of the referee 1 : "For example, it would be nice if the authors would state how long it takes to run the matlab code for some of the cases at different spatial resolutions (perhaps in a table). Surely, it is much faster than LES."

In the revised manuscript, we add the Tab 1. We add this paragraph in section 4.4.1 (Effects of numerical resolution):

Table 1 shows the time step, process time for one time step and process time for 2h-simulation with 3DCLOUD model, as a function of the numerical resolution. DYCOMS2-RF01 and BOMEX cases are presented. The process time for 2h-simulation is indicated because 3DCLOUD algorithm convergence is achieved after 2 h (or less) of simulation for stratocumulus, cumulus and cirrus regimes (see Fig. 10 for cumulus case). For both cases, the smaller the spatial resolution, the smaller the step time and the larger the process time. A comparison between 3DCLOUD and BRAMS LES computation time for a specific DYCOMS2-RF01 case is added (see Sect. 3.4). For this specific case, 3DCLOUD simulation is thirty times faster than BRAMS simulation. Note that 3DCLOUD (Matlab code) runs on a personal computer with Intel Xeon E5520 (2.26 GHz) and BRAMS (Fortran code) runs on a PowerEdge R720 with Intel Xeon E5-2670 (2.60 GHz), both of them having a single-processor configuration.

Table 1. Time step, process time for one time step and process time for 2h-simulation with 3DCLOUD model, as a function of the numerical resolution. DYCOMS2-RF01 and BOMEX cases are presented. A comparison between 3DCLOUD and BRAMS LES computation time for a specific DYCOMS2-RF01 case is added. 3DCLOUD (Matlab code) runs on a personal computer with Intel Xeon E5520 (2.26 Ghz) and BRAMS (Fortran code) runs on a PowerEdge R720 with Intel Xeon E5-2670 (2.60Ghz), both of them having a single-processor configuration.

Study case	Point mesh $N_x \times N_y \times N_z$	Horizontal numerical resolution Δx [m]	Time step [s]	Process time [s]	Process time for 2h-simulation [s]
DYCOMS2-RF01	$50 \times 50 \times 50$	200	10	0.4	290
	$100 \times 100 \times 50$	100	7	1.3	1340
	$200 \times 200 \times 50$	50	5	5	7200
	$400 \times 400 \times 50$	25	3	18	43200
BOMEX	$50 \times 50 \times 70$	200	30	0.7	170
	$100 \times 100 \times 70$	100	25	2.5	720
	$200 \times 200 \times 70$	50	20	10	3600
	$400 \times 400 \times 70$	25	14	40	20600
DYCOMS2-RF01					
3DCLOUD	$100 \times 100 \times 100$	40	13	2.7	1500
BRAMS	$100 \times 100 \times 100$	40	0.3	2	48600

4. How many iterations did 3DCloud require in order to produce Figs. 7, 8, and 11?

We used 700 iterations in order to produce Figs 7 and 1000 iterations in order to produce Figs 11. In order to simulate Figs.8, we let 3DCLOUD iterate until 2h-simulation is done.

We add this information in figure captions in the revised manuscript.

Technical Comments:

The article needs to be proofread more thoroughly. Below are three examples of errors from the first two pages, but many more errors are contained in the following pages.
Abstract: "3DCLOUD model was developed to run on a personnel computer"
p. 297, lines 13–14: "These biases are at least, function of the cloud coverage and of the variability of cloud optical depth or water content."
p. 297, lines 18–20: "Determining the significance of the 3-D inhomogeneity of clouds for climate and remote sensing applications requires to measure and to simulate the full range of actual cloud structure."

The revised manuscript has been proofread by a native English speaker.